Medical Engineering and Physics 73 (2019) 1–8

Contents lists available at ScienceDirect

Medical Engineering and Physics

journal homepage: www.elsevier.com/locate/medengphy

Protocol development for synchrotron contrast-enhanced CT of human hip cartilage

Honglin Zhang[a], George Belev[b,1], Rachel C. Stewart[c], Mark W. Grinstaff[c], Brian D. Snyder[d], David R. Wilson[a,*]

[a] Department of Orthopaedics, University of British Columbia, Centre for Hip Health and Mobility, 2635 Laurel St, Vancouver BC V5Z 1M9, Canada
[b] Canadian Light Source, 44 Innovation Blvd, Saskatoon, SK S7N 2V3, Canada
[c] Departments of Biomedical Engineering and Chemistry, Boston University, 403-44 Cummington Mall, Boston, MA 02215, USA
[d] Center for Advanced Orthopaedic Studies, Beth Israel Deaconess Medical Center, Harvard Medical School, 330 Brookline Ave., RN 115, Boston, MA 02215, USA

ARTICLE INFO

Article history:
Received 22 February 2019
Revised 11 July 2019
Accepted 21 August 2019

Keywords:
Hip
Cartilage
Strain
Osteoarthritis
Mechanics
Contrast agent
Computed tomography
Synchrotron

ABSTRACT

Understanding hip osteoarthritis requires new investigational tools for quantitative studies of biophysical and biomechanical properties as well as for determination of structure. Three new protocols to study pathological changes in cartilage and to measure cartilage thickness in intact human hips are described using synchrotron contrast enhanced computed tomography (sCECT) with the iodinated contrast agent CA4+. Ten human cadaver hips were prepared and injected with CA4+ using three different methods, all of which included rotation and distraction of the joint. CA4+ diffusion into cartilage was monitored using sCECT. The thickness of acetabular and femoral cartilage was also measured. Diffusion times ranged from 2 h to 75 h, depending on the injection protocol and the cartilage region. Direct single injection of the contrast through the labrum resulted in the fastest diffusion times. The iodine attenuation coefficient, which reflects the contrast agent distribution in the cartilage, ranged from 0.0142/cm to 0.1457/cm. Three injections at the head/neck conjunction area yielded the highest iodine attenuation coefficients in cartilage. The femoral cartilage in the Superior-Medial compartment was significantly thicker than in the other 3 femoral compartments, and femoral cartilage in the Superior-Anterior compartment was significantly thinner than the other 3 femoral compartments. The acetabular cartilage in the Superior compartment was significantly thicker than that in the Superior-Posterior compartment. sCECT with CA4+ allows assessment of hip cartilage thickness with 0.1 mm isotropic voxel size, sufficient for evaluating cartilage pathology and biomechanics.

1. Introduction

Hip osteoarthritis (OA), a leading cause of pain and disability, affects 3% of the population aged 55 to 74 years old [1]. It develops over time, often as a consequence of deformity or injury, with a cascade of biochemical and biomechanical processes leading to degeneration of the articular cartilage and other joint tissues. Thus, characterizing, quantifying, and understanding hip cartilage degeneration is of considerable interest. Additionally, gaining further insight into hip mechanics and the relationship between mechanics and hip osteoarthritis is of interest because abnormal mechanics is widely thought to be a cause of many cases of hip OA [2].

Medical imaging is widely used to study cartilage degeneration of articulating joints. Magnetic resonance imaging (MRI) protocols, such as dGEMRIC, T1ρ, and T2, assess changes in cartilage that are associated with early cartilage degeneration as a result of structural or biochemical alterations [3]. From a biomechanics perspective, MRI has also been used to quantify cartilage strain in intact loaded knee joints [4] and hip joints [5,6] using measures of cartilage thickness before and after joint loading. A limitation of MRI approaches is that quantifying regional differences in cartilage strain accurately requires long scan times and high field strengths.

Contrast-enhanced computed tomography (CECT) is also used to study early cartilage degeneration and joint mechanics. CECT relies on a contrast agent to increase visibility of cartilage from the bone and synovial space enabling accurate measurement of cartilage thickness. Additionally, CECT with charged iodinated contrast

* Corresponding author.
E-mail address: david.wilson@ubc.ca (D.R. Wilson).
[1] Present affiliation: Saskatchewan Structural Sciences Center, University of Saskatchewan, Rm. G81 Thorvaldson Building, 110 Science Place, Saskatoon, SK, S7N 5C9, Canada

https://doi.org/10.1016/j.medengphy.2019.08.003
1350-4533/

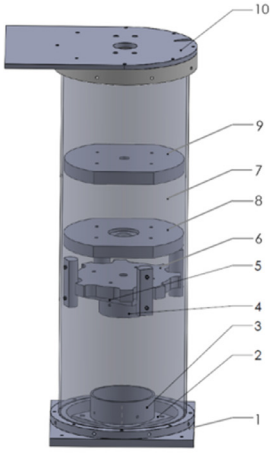

ITEM NO.	PART NUMBER	QTY.
1	Base	1
2	Pelvis Potting and Diffusion Plate	1
3	Pelvis Potting Tube	1
4	Femur Potting Tube	1
5	Femur Potting and Diffusion Plate	1
6	Plate 1 (potting to load cell)	1
7	tubeAssembly	1
	Tube (with holes)	1
	Rail	4
	Top Lip (weld to tube)	1
8	Plate 2 (load cell to spring)	1
9	Plate 3 (spring to bearing)	1
10	Diffusion Lid	1

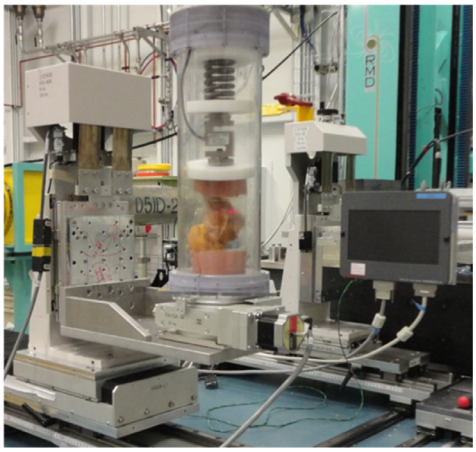

A B C

Fig. 1. A. A prepared cadaver hip joint showing the injection location for method I and method II & III. B. Schematic diagram of the diffusion rig. C. Imaging system setup with cadaveric hip in the diffusion rig at the BMIT-BM beamline at the Canadian Light Source.

agents (either anionic or cationic) provides quantification of glycosaminoglycan (GAG) concentration and distribution within cartilage [7–9]. GAGs play an important structural and biomechanical role in the cartilage matrix. Anionic contrast agents accumulate in cartilage in inverse relationship to GAG concentration, because GAGs are negatively charged. Cationic contrast agents accumulate in direct proportion to the concentration of GAGs. The cationic contrast agent, CA4+ (possessing four positive amine groups) is superior to anionic agents for quantification of GAG content [10,11]. Significant correlations between CECT attenuation and GAG concentration as well as mechanical stiffness have been reported in knee cartilage plugs [10–13], human MCP joints [14], and in human intact knees [15,16].

Synchrotron imaging provides a unique opportunity to apply CECT imaging to study GAG distribution and cartilage strain in intact human hips. Synchrotrons produce high intensity X-rays with high collimation and a wide spectrum, and produce the high resolution images (<100 µm) required to measure physiological levels of cartilage strain. Importantly, synchrotrons do not have the sample size restrictions of the microCT devices that are widely used for CECT [16,17], allowing intact hip joints to be imaged within devices loading them to physiological levels – a significant advantage. The BioMedical Imaging and Therapy (BMIT) beamline at the Canadian Light Source (CLS) is designed to image biological tissues [18] in a large range of sizes and is ideal for investigation of intact hips.

Applying synchrotron CECT (sCECT) to study the intact human hip requires a protocol for delivery of contrast agent into the hip cartilage and quantification of the diffusion time. Achieving full diffusion of contrast agent into the intact human hip is particularly challenging because the joint is sealed by the acetabular labrum and because a substantial portion of the cartilage surfaces are in contact with each other in a resting posture. Consequently, our study objectives are to:

- Develop a sCECT imaging protocol for intact cadaver hips;
- Develop and assess CA4+ injection and diffusion protocols for intact cadaver hips;
- Determine the diffusion time of CA4+ into the cartilage layers of intact cadaver hips; and,
- Assess the feasibility of measuring cartilage thickness using sCECT imaging

2. Methods

2.1. Specimens and preparation

Ten hips were obtained from 5 full pelvis to proximal femur cadaver specimens (aged 34–65 years, mean 53 years; 2 male, 3 female; weighed 65 ±15 kg) obtained from the Life Legacy Foundation (Tucson, AZ, USA). All specimens were scanned using helical CT (Toshiba Aquilion; Tustin, CA, USA) with a slice thickness of 0.5 mm and an in plane resolution of 0.72 mm. Hip joint coordinate systems were defined using an established protocol [19] based on landmarks (PSIS-Posterior Superior Iliac Spine, ASIS-Anterior Superior Iliac Spine, femoral head center, and acetabular socket center) identified on these CT scans, the orientation of the femoral neck and shaft in the images, and estimation of the midpoint of the epicondylar line of the knee according to the gender and height of the donor [20].

Each specimen was thawed and dissected to the level of the joint capsule, and then the pelvis and femoral shaft were potted in dental cement so that the specimen could later be mounted in a loading rig (Fig. 1A). All procedures were approved by our institution's clinical research ethics board.

2.2. Contrast agent diffusion protocol

We designed and built a "diffusion rig" to apply cyclic compression and distraction to the hip joint to speed up diffusion of the contrast agent into the cartilage (Fig. 1B). Our motivation for building this rig was that early trials had shown that contrast agent did not reach an equilibrium concentration in the cartilage after 20 h in a static hip. The rig is driven by a motor in a rack and pinion system (Oriental Motor U.S.A. Corp., Torrance, CA, USA) and force is measured with an S-type load cell (HSI-S, Panther). The magnitude of the applied force and loading rate was controlled by custom LabVIEW code (LabVIEW, National Instruments, Austin, TX, USA).

We injected CA4+ into each specimen with a 22G1 needle (Becton Dickinson & Co, Franklin Lakes, NJ, USA). Injection continued until resistance from the needle and bulging of the joint capsule indicated full injection, with reference to normal human hip joint capacity (8 to 20 mL depending on the size of the joint [21]). We assessed 3 injection methods to study the effects of injection protocol on CA4+ diffusion into cartilage:

Table 1A
Details of injection, imaging, and diffusion for each specimen.

Donor #	Side	Injection	Vertical coverage	Diffusion time
#1	L	I,	25 mm	14h04m
	R	18.5ml		15h22m
#2	L	II,	48.4mm	45h34m
	R	18ml		33h15m
#3	L			31h23m
	R			40h26m
#4	L	III,	36 mm	31h10m
	R	Table 1B		27h25m
#5	L			30h30m
	R			31h55m

Table 1B
Timing of multiple injections and volume of injected CA4+ for 4 specimens.

#4	Time	0h0m	12h10min	18h30m
L	Amount	17 ml	10 ml	15 ml
#4	Time	0h0m	12h45m	18h20m
R	Amount	20 ml	12 ml	6 ml
#5	Time	0h0m	7h55min	13h41min
L	Amount	20 ml	11 ml	10 ml
#5	Time	0h0m	8h20min	18h15min
R	Amount	20 ml	20 ml	16.5 ml

I. Single injection of contrast agent into the intra-articular space through the labrum (2 specimens, Table 1A, Fig. 1A).
II. Single injection of contrast agent at the anterior conjunction area of femoral head and neck, corresponding to clinical hip arthrography (4 specimens, Table 1B, Fig. 1A).
III. Three injections (spaced over the imaging time) at the anterior conjunction of the femoral head and neck (4 specimens, Table 1A, Fig. 1A).

After each injection of CA4+, we performed 100 manual rotations of the hip to speed up diffusion of the contrast agent. Specimens were then wrapped in gauze soaked in phosphate-buffered saline (PBS+) to prevent dehydration and mounted upside down in the diffusion rig. After each image acquisition, the rig was used to apply a ±30 N cyclic superior/inferior load to the hip for 30 min at a frequency of 0.025 Hz. The cyclic loading was selected to distract the hip sufficiently to allow contrast agent to flow through the labrum seal, while not damaging the joint and the cartilage surface.

2.3. Synchrotron imaging

Synchrotron CT imaging was done on the BioMedical Imaging and Therapy Bending Magnet (BMIT-BM, 05B1-1) beamline at the Canadian Light Source (CLS) (Fig. 1B). We used a rectangular filtered white beam controlled by a fast shutter that measures 245 mm horizontally and 2.8 mm vertically. The beam passed through a 6.2 mm copper filter before reaching the specimen to remove lower energy X-rays and improve image quality by decreasing X-ray scatter. The spectrum of the imaging beam is shown in Fig. 2. The specimen was placed on a rotational stage (Thorlabs NR360 S/M, Thorlans Inc., Newton, NJ, USA), which rotated 180° at 12°/sec during imaging at 25.5 m from the light source, yielding 1200 different projections used to reconstruct the images in 3D. The projections were collected at every 0.15° rotation with a CMOS flat panel sensor, C9252DK-14, HAMAMATSU (Hamamatsu Corporation, Hamamatsu City, Shizuoka Pref., Japan), working in partial scan mode with a pixel size of 0.1 mm at 26 m from the light source. We repeated this procedure with the beam at different vertical positions relative to the hip to obtain full coverage of the joint. Before each collection of CT projections (I), we took a dark image without the specimen in the beam and with the shutter off to measure the environmental noise and we took a flat image (I_0) without the specimen in the beam but with the shutter on to normalize the projections in CT collection and to correct the defects in the detector and the spatial and temporal variation of the beam intensities.

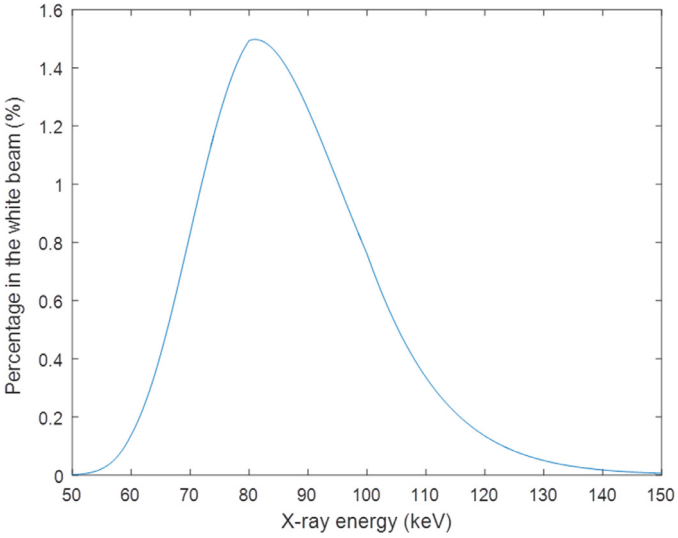

Fig. 2. Imaging beam spectrum.

2.4. Data analysis

The attenuation coefficient was obtained from the projections. The signal in each pixel of the CT projection, I, can be expressed as:

$$I = I_0 e^{-\mu t}$$

where I_0 is the flat image collected when there is no object in the beam, μ is the linear attenuation coefficient of the object in the beam, and t is the thickness of the object. The attenuation coefficient of the object was found from:

$$\mu = -ln\frac{I}{I_0}/t$$

The dark image was subtracted from both I and I_0 images to reduce environmental noise. The CT cross-sectional images were obtained by filtered back projection through the inverse Radon transform in Matlab (Mathworks; Natick, MA, USA) with the attenuation coefficient (μ) as the signal of the voxel with a unit of 1/cm. This CT reconstruction was applied to all data sets.

For cartilage and diffused iodine, $\mu = \mu_C + \mu_I$, where μ_C is the attenuation coefficient of cartilage and μ_I is that of diffused iodine, which is proportional to the concentration of iodine in the cartilage. μ_I was calculated by subtracting μ_C obtained from the pre-injection scan of the cartilage.

After CT reconstruction, images of the femur and pelvis collected at different time points were aligned using 3D voxel registration (Analyze 10, AnalyzeDirect Inc., Overland Park, KS, USA).

The femoral and acetabular cartilage layers were then segmented on a volume created by subtracting the pre-injection volume from the most diffused one. Cartilage was segmented manually (Analyze 10, AnalyzeDirect Inc., Overland Park, KS, USA) every few slices from this resulting volume and then the remaining slices were auto connected and smoothed (3D Slicer 4.8 [22]).

To visualize the distribution of iodine in the cartilage and the thickness of the cartilage layers, a 2D projection map was

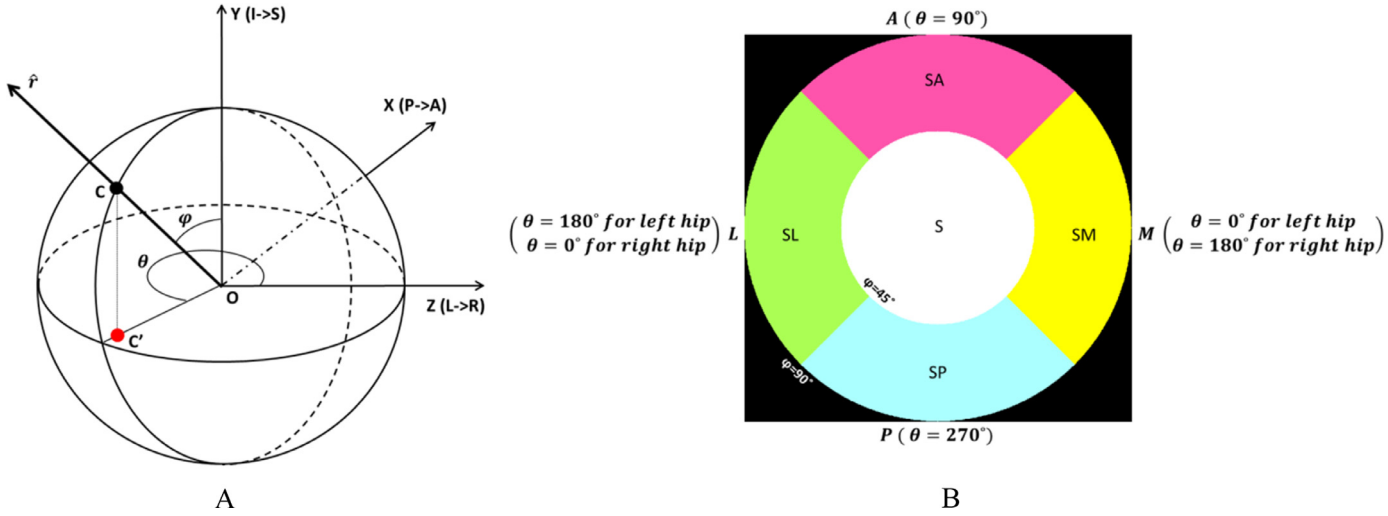

Fig. 3. 2D visualization of spherical 3D cartilage data. A. A spherical coordinate system with origin at the sphere center corresponding to the femoral head center for femoral cartilage and acetabular center for acetabular cartilage. X is the posterior to anterior direction, Y is from inferior to superior, and Z points from left to right. Any point on the surface of the sphere can be represented by azimuth angle θ and zenith angle φ. B. 2D map of cartilage layers with pixels defined by (θ, φ) and the superior part of the cartilage located at the center. 5 compartments are shown here, representing φ from 0° to 90°.

Table 2
Equilibrium time t_e (hour) for each compartment of the cartilage layers of the specimens injected with method I and method II. The *t*-test compares equilibrium time for injection method I and injection method II.

Injection method	Specimen	Femoral cartilage				Acetabular cartilage	
		S	SA	SP	SM	S	SP
I	#1 L	11.89	8.24	4.46	9.41	9.47	6.89
	#1 R	7.07	–	2.25	7.43	5.96	5.51
II	#2 L	56.52	3.47	26.17	25.84	75.64	47.71
	#2 R	13.16	2.03	12.66	14.96	25.39	19.53
	#3 L	9.51	11.17	2.84	17.06	–	–
	#3 R	17.07	9.73	22.69	27.50	16.18	16.80
t-test *p* value ($\alpha = 0.05$)		0.21	0.38	0.09	0.03	0.14	0.09

developed [23]. A spherical coordinate system was set up in the same way as the joint coordinates (Fig. 3). The origin O was defined as the femoral head center for the femoral cartilage layer and as the center of the acetabular socket for the acetabular cartilage layer. The orientation of the specimen in the synchrotron CT was found by registering the clinical CT image (in which we had defined the coordinate system) to the synchrotron CT image. The zenith angle φ was measured from the foot-head direction Y. The azimuth angle θ was measured from the left-right direction Z. 2D maps were created with the center corresponding to the superior point on the cartilage layer and pixels corresponding to points on the cartilage layer defined by (θ, φ) (Fig. 3B). The hip cartilage layers were divided into 9 compartments: Superior (S), Superior-Anterior (SA), Superior-Posterior (SP), Superior-Medial (SM), Superior-Lateral (SL), Inferior-Anterior (IA), Inferior-Posterior (IP), Inferior-Medial (IM), and Inferior-Lateral (IL) [24]. In this project, we studied 5 compartments: S, SA, SP, SM, and SL.

Diffusion data were fitted to a curve in the form of $\mu_{I0}[1\text{-}exp(-t/\tau)]$, where μ_{I0} is the iodine attenuation coefficient when the CA4+ is fully diffused into the cartilage, t is diffusion time after injection, and τ is the diffusion time constant, the time required to reach 63.2% of the attenuation at equilibrium time t_e (defined as when 95% of μ_{I0} is reached) [25,26]. τ of each compartment of each hip was calculated with the averaged attenuation coefficient of each compartment if the cartilage covered more than 1/4 of the compartment area in the image. t_e was calculated using $t_e = 3\tau$ for each region in each hip. We used the fitted diffusion functions to calculate the iodine attenuation coefficient at 30 h for specimens injected with method I and II. Interpolation was used to determine the iodine attenuation coefficient at 30 h if there was no image acquisition at the time for the specimens injected with method III. Measurements of averaged iodine attenuation and equilibrium times were compared between injection methods using a pooled *t*-test [27].

The thickness of femoral and acetabular cartilage was measured on the most diffused volume and reported in 2D maps. The cartilage thickness measured in the image was multiplied by a correction factor of 0.98 due to the distance between the specimen and the detector.

3. Results

Equilibrium times (t_e - calculated by curve fitting) varied substantially by compartment, injection method and specimen, ranging from 2.0 to 75.6 h (Table 2). The equilibrium times were significantly longer for a single injection at the head/neck conjunction (method II) compared to a single injection through the labrum (method I) for femoral compartment SM ($p = 0.03$) (Table 2). We found no difference in the equilibrium times for femoral compartment SA ($p = 0.38$) between the two methods. We did not calculate the diffusion curves and equilibrium time for 3 injections at the head/neck conjunction (method III) because multiple injections complicate the diffusion curve compared to the single injection procedures.

We observed qualitative differences in diffusion patterns between the three injection methods. For direct single injection of

Table 3
Iodine attenuation coefficients (1/cm) for each compartment of each specimen after 30 h of diffusion for the three different injection methods. The *t*-test compares the iodine attenuation coefficients among different injection methods for different cartilage compartments.

Injection method	Specimen	Femoral cartilage				Acetabular cartilage	
		S	SA	SP	SM	S	SP
I	#1 L	0.1079	0.083	0.0781	0.0404	0.0795	0.0956
	#1 R	0.0700	–	0.0653	0.0338	0.0555	0.0765
II	#2 L	0.0394	0.1133	0.0604	0.0765	0.0172	0.0345
	#2 R	0.0592	0.0847	0.0634	0.0617	0.0419	0.0533
	#3 L	0.0195	0.0639	0.0186	0.0142	–	–
	#3 R	0.0549	0.1092	0.0460	0.0375	0.0268	0.0440
III	#4 L	0.1100	0.1390	0.1038	0.1077	0.0929	0.1050
	#4 R	0.1439	0.1457	0.1291	0.1327	0.1237	0.1186
	#5 L	0.0946	0.1225	0.1140	0.1073	0.0762	0.1033
	#5 R	0.0964	0.1424	0.1169	0.0772	0.0585	0.1249
t-test *p* value ($\alpha = 0.05$)	Method I>Method II	0.03	0.36	0.10	0.32	0.03	0.01
	Method I<Method III	0.17	0.009	0.004	0.008	0.20	0.03
	Method II<Method III	0.002	0.006	0.0005	0.008	0.01	0.0001

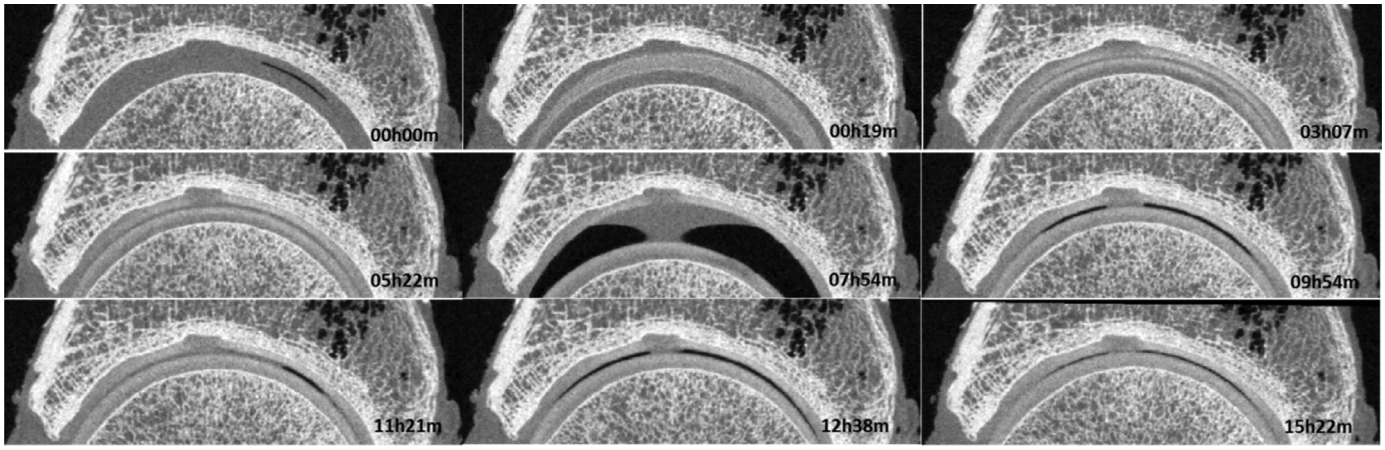

Fig. 4. One vertical slice of specimen #1 (right hip) at nine time points after injection of CA4+ through the labrum. Both cartilage layers had direct contact with CA4+ immediately after injection. As CA4+ diffused into the joint, the interface between acetabular and femoral cartilage became visible. The image obtained at 07h54m after injection has a large joint space because the distraction force was not removed completely for that image.

CA4+ through the labrum (method I), femoral cartilage diffusion started in the superior lateral compartment (Fig. 5). Acetabular cartilage diffusion started in the region around the fossa and CA4+ reached the highest concentration in this area (Fig. 5). For a single injection of CA4+ at the anterior head-neck conjunction (method II), diffusion started from the SA compartment for femoral cartilage and from the region around the acetabular fossa for acetabular cartilage (Fig. 6). Diffusion of CA4+ continued in femoral regions inside the acetabulum much longer than in regions outside. This indicates that CA4+ was successfully injected into the hip joint capsule but did not reach the inside of the acetabular socket. For three separate injections at the anterior head-neck conjunction area (method III), there was limited diffusion of CA4+ into the acetabular socket covered cartilage layers after the 1st injection, some diffusion after the 2nd injection, and further diffusion after the 3rd injection (Fig. 7).

The attenuation coefficient of iodine in the cartilage, which is proportional to the amount of contrast agent diffused into the cartilage, varied from 0.0142/cm to 0.1457/cm 30 h after injection depending on the compartment, injection method, and specimen (Table 3). The iodine attenuation coefficients are significantly higher for a single injection through labrum (method I) compared to a single injection at the head/neck conjunction (method II) at femoral compartment S ($p = 0.03$) and acetabular compartments S ($p = 0.03$) and SP ($p = 0.01$). 3 injections at the head/neck conjunction (method III) increased the iodine attenuation coefficient significantly in almost all cartilage compartments (all $p<=0.03$) compared to single injection through labrum (method I), except the S compartments in both femoral and acetabular cartilage. Compared to method II, method III increased the iodine attenuation coefficient significantly in all compartments of cartilage layers (all $p<=0.01$).

Cartilage thickness could be measured because injecting CA4+ made the interface between acetabular and femoral cartilage visible (Fig. 4). In these 10 hips, the femoral cartilage in the SM compartment was significantly thicker than that in the other 3 femoral compartments (Table 4A and 4B), and femoral cartilage in the SA compartment was significantly thinner than the other 3 femoral compartments. The acetabular cartilage in the S compartment was significantly thicker than the acetabular cartilage in the SP compartment.

4. Discussion

The key findings from this work are: a) movement and loading of the hip are essential to ensuring diffusion of contrast agent into hip cartilage; b) diffusion characteristics substantially vary for cadaver hip cartilage and depend on injection protocol and cartilage region; and, c) all injection methods afforded sufficient contrast agent diffusion into the hip cartilage to measure cartilage thickness using sCECT imaging.

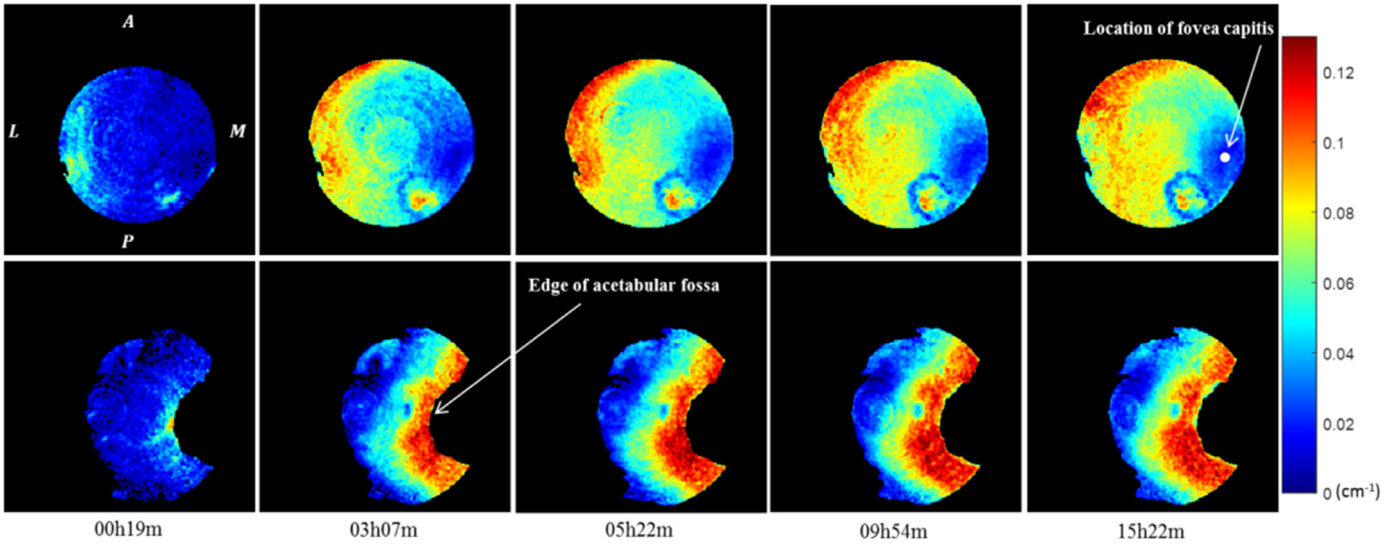

Fig. 5. 2D maps of cartilage attenuation at 5 selected diffusion time points for specimen #1 right in which the injection method I, injecting directly through the labrum, was applied. The top row is femoral cartilage in which the fovea capitis is located around the white dot in the maps and the bottom row is acetabular cartilage in which the medial side edge indicates the start of the acetabular fossa.

Table 4A
Thickness (mm) of cartilage for each compartment for all specimens.

ID and side	Femoral cartilage				Acetabular cartilage	
	S	SA	SP	SM	S	SP
#1 L	1.87	1.24	1.37	2.68	2.00	1.24
#1 R	1.99	–	1.71	3.09	1.78	1.18
#2 L	1.34	0.96	1.24	1.45	1.63	1.06
#2 R	1.35	0.93	1.24	1.69	1.47	0.98
#3 L	1.07	1.04	1.13	1.16	–	–
#3 R	1.42	1.27	1.31	1.48	1.33	1.08
#4 L	1.48	0.96	1.44	1.88	1.20	1.10
#4 R	1.44	0.99	1.37	2.00	1.06	1.02
#5 L	1.00	1.26	0.99	1.00	0.87	0.89
#5 R	0.99	1.11	1.10	1.05	1.53	1.24
Mean	1.40	1.08	1.29	1.75	1.43	1.09
Std	0.34	0.14	0.20	0.69	0.36	0.12

Table 4B
T test of cartilage thickness among different cartilage compartments in 10 hips.

t-test *p* value ($\alpha = 0.05$)		Femoral cartilage			Acetabular cartilage	
		SA	SP	SM	S	SP
Femoral cartilage	S	0.01	0.20	0.08	0.41	0.01
	SA	–	0.01	0.006	0.008	0.48
	SP	–	–	0.03	0.15	0.009
	SM	–	–	–	0.12	0.006
Acetabular cartilage	S	–	–	–	–	0.007

In most of the hips, the femoral cartilage was thickest around the fovea capitis and thinner away from it, and the acetabular cartilage was thinnest around the acetabular fossa and thicker away from it. This general pattern of cartilage thickness is consistent with the findings from two anatomical studies [28,29]. Given that the voxel size ($0.1 \times 0.1 \times 0.1$ mm) was substantially smaller than that of clinical CT and MRI (typically 0.3 mm or larger), this technique allows detection of smaller pathological differences in cartilage (e.g., small cartilage defects, early cartilage thinning) or strains in response to physiological levels of mechanical compression [5].

It was not surprising that, in general, diffusion was more rapid (2 h for SA compartment of femoral cartilage of #2 right hip) in regions where the contrast agent was in direct contact with cartilage, since diffusion across the cartilage surface is relatively fast. The reported diffusion time for CA4+ reaching equilibrium ranges from less than 1 h for in vivo rabbit femoral groove cartilage [26] to 37.5 h for ex vivo bovine femoral groove cartilage plugs [30]. The challenge of delivering contrast agent to intact human hip cartilage is that the labrum is a seal that inhibits movement of fluid in and out of the hip joint. Thus, delivering contrast agent within the labral seal is critical. Rotating and distracting the hip helped to move contrast agent within joint. Our observation that, in some regions, the attenuation decreased somewhat after an initial rapid increase (Figs. 5–7) suggests that contrast agent was diffusing within cartilage, and that this process was slower than diffusion across the cartilage surface.

The choice of injection method was also dictated by the amount of soft tissue on the specimen. Direct single injection of CA4+ through the labrum (Injection method I) was challenging because it was difficult to navigate the needle into the intraarticular space. However, it yielded the shortest diffusion time, likely because all of the cartilage was in direct contact with contrast agent. This method was best suited to specimens that had most of the soft tissue removed. A single injection of CA4+ at the anterior head-neck conjunction (Injection method II) was easier to perform but yielded a much longer diffusion time, likely because the contrast agent must travel to the intraarticular space by convection. Injecting at the anterior femoral head and neck conjunction area 3 times (Injection method III), increased the concentration of contrast in the cartilage because more CA4+ was injected, but did not increase diffusion. Injection methods II and III are more practical for specimens with intact soft tissue or for live patients.

The distribution of contrast agent in the cartilage must be interpreted with caution in the hip because the labrum interferes with continuous, direct contact between the contrast agent and the cartilage surface. Even with direct single injection of CA4+ through the labrum (Injection method I), the contrast agent frequently leaked through the labrum and did not re-diffuse back into the joint space. This is an important finding because CECT imaging using CA4+ is used as a surrogate to map glycosaminoglycan concentration [11,14,26,31] and cartilage stiffness [16]. To use CA4+ CECT for quantification of hip GAG concentration, the joint should be disarticulated and the joint surfaces should be exposed and immersed in the contrast agent to reach diffusion equilibrium.

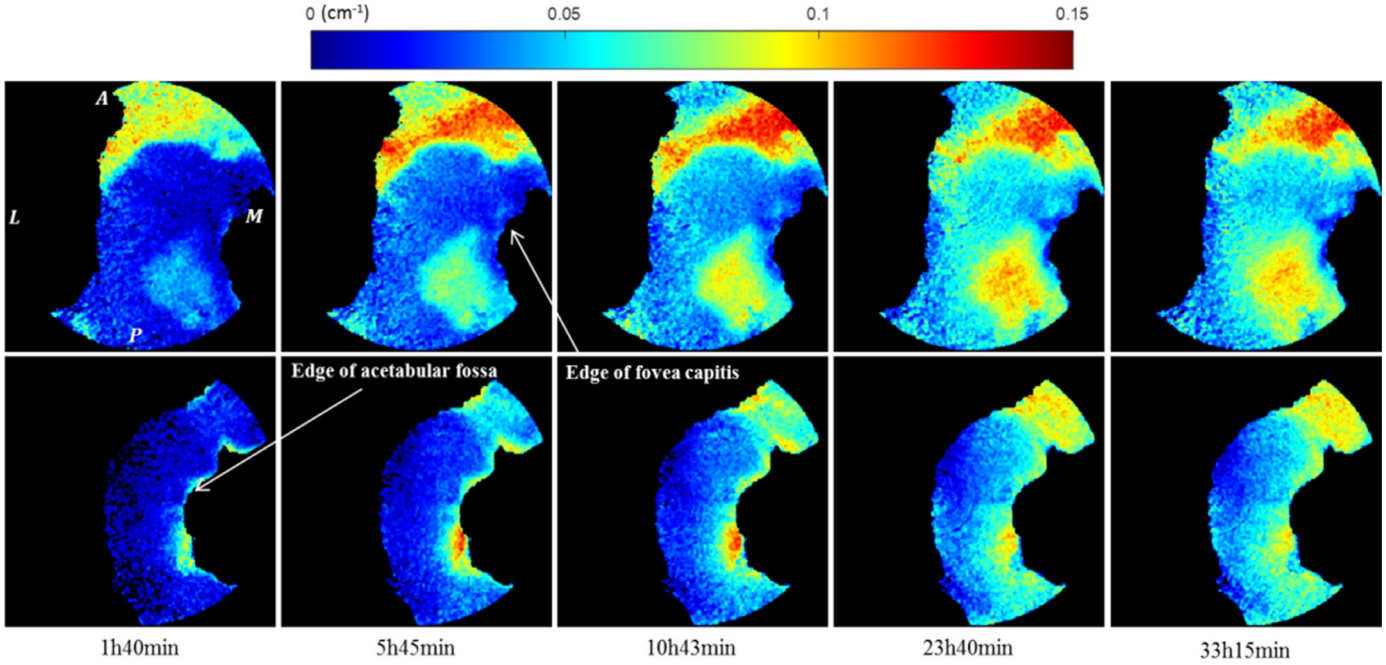

Fig. 6. 2D diffusion maps at 5 selected time points of #2 right hip cartilage for injection method II, a single injection of CA4+ at the anterior head neck conjunction. The top row is femoral cartilage and the bottom row is acetabular cartilage.

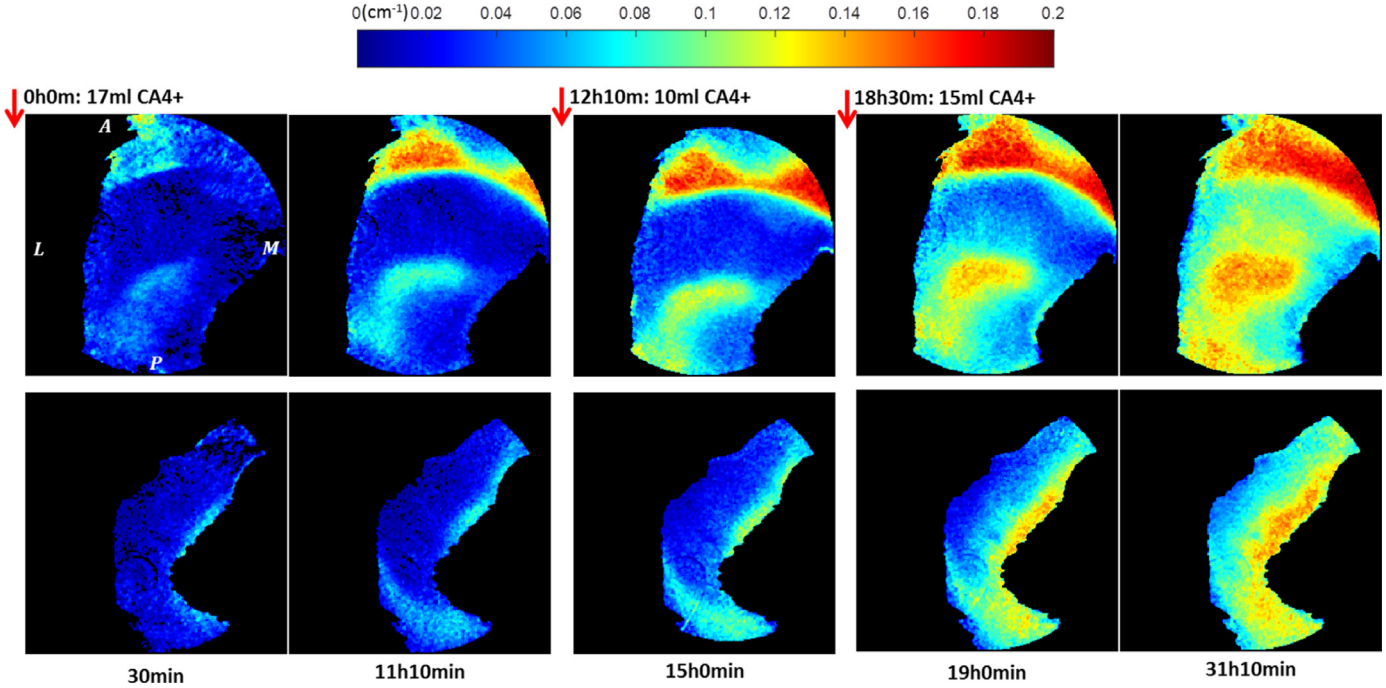

Fig. 7. 2D diffusion maps at 5 selected diffusion time points of #4 left hip cartilage for injection method III, 3 injections of CA4+ at the anterior head neck conjunction. The top row is femoral cartilage and the bottom row is acetabular cartilage. After the 1st and 2nd injections there was limited uptake of CA4+ inside of the acetabular socket. There was much more CA4+ uptake inside the acetabular socket after the 3rd injection.

The advantages of this approach are that sCECT provides a tool to image the intact human hip in a loading device and to measure cartilage thickness with a voxel size of 0.1 mm, which is sufficient to measure small pathological changes in cartilage thickness and physiological levels of cartilage strain. Greaves et al. [5] reported an average cartilage deformation in the hip joint was 0.96 ± 0.27 mm after 225 min of axial loading of 1980 N (2.3 times of body weight). One limitation of the approach is the imaging time, which was about 35 min for each CT. This is important to consider due to the time-dependent mechanical behavior of cartilage. Imaging time was dictated, to a large extent, by the data acquisition system which included the detector, the frame grabber, the computer, and the control software. The imaging time can be improved substantially by changing the detector system or switching to another beamline. Another limitation is the need for access to a synchrotron for the imaging. A further limitation is that, due to the imaging time and radiation involved, this approach could not be used in vivo. However the method does represent substantial

progress in ex vivo assessments of hip mechanics and has many potential applications in assessing hip disease and treatments.

5. Conclusions

sCECT with CA4+ allows assessment of hip cartilage thickness with 0.1 mm isotropic voxel size. Successful imaging requires delivery of CA4+ into the intraarticular space, which was evaluated using three administration routes. Direct single injection of the contrast through the labrum is the preferred approach as this ensured the greatest contact of the agent with the cartilage, and results in the fastest diffusion times. The developed protocol for sCECT can be applied to: 1) detect small defects in cartilage; 2) measure the thickness of cartilage layers and the distribution of strains; 3) determine the mechanical properties of cartilage; and 4) characterize and quantify the degeneration of the articular cartilage. Importantly, sCECT with CA4+ technique provides sufficient resolution to empower the study of cartilage pathology and biomechanics.

Funding

Research described in this paper was funded by the Natural Sciences and Engineering Research Council of Canada (Discovery Grant #05246). Research was performed at the Canadian Light Source, which is funded by the Canada Foundation for Innovation, the Natural Sciences and Engineering Research Council of Canada, the National Research Council Canada, the Canadian Institutes of Health Research, the Government of Saskatchewan, Western Economic Diversification Canada, and the University of Saskatchewan.

Ethical approval

Ethical approvals for this study were granted by the Clinical Research Ethics Board of the University of British Columbia (H10-00699) and the Biomedical Research Ethics Board of the University of Saskatchewan (Bio10-51).

Declaration of Competing Interest

None declared.

Supplementary materials

Supplementary material associated with this article can be found, in the online version, at doi:10.1016/j.medengphy.2019.08.003.

References

[1] Bijlsma JWJ. Strategies for the prevention and management of osteoarthritis of the hip and knee. Best Pract Res Clin Rheumatol 2007;21(I):59–76.
[2] Ganz R, Parvizi J, Beck M, Leunig M, Notzli H, Siebenrock KA. Femoroacetabular impingement: a cause for osteoarthritis of the hip. Clin Orthop 2003;417:112–20.
[3] Burstein D, Gray ML. Is MRI fulfilling its promise for molecular imaging of cartilage in arthritis? OsteoArthr Cartil 2006;14:1087–90.
[4] Song Y, Greve JM, Carter DR, Koo S, Giori NJ. Articular cartilage MR imaging and thickness mapping of a loaded knee joint before and after meniscectomy. Osteoarthr Cartil 2006;14(8):728–37.
[5] Greaves LL, Gilbart MK, Yung A, Kozlowski P, Wilson DR. Deformation and recovery of cartilage in the intact hip under physiological loads using 7T MRI. J Biomech 2009;42(3):349–54.
[6] Greaves LL, Gilbart MK, Yung AC, Kozlowski P, Wilson DR. Effect of acetabular labral tears, repair and resection on hip cartilage strain: A 7T MR study. J Biomech 2010;43(5):858–63.
[7] S R, Grushko G, Maroudas A. Some biochemical and biophysical parameters for the study of the pathogenesis of osteoarthritis: a comparison between the processes of aging and degeneration in human hip cartilage. Connect Tissue Res 1989;19(2–4):149–76.
[8] Christensen SB, Reimann I. Differential histochemical staining of glycosaminoglycans in the matrix of osteoarthritic cartilage. Acta Pathol Microbiol Scand Sect A Pathol 1980;88 A(1–6):61–8.
[9] Lorenzo P, Bayliss MT, Heinegård D. Altered patterns and synthesis of extracellular matrix macromolecules in early osteoarthritis. Matrix Biol 2004;23(6):381–91.
[10] Joshi NS, Bansal PN, Stewart RC, Snyder BD, Grinstaff MW. Effect of contrast agent charge on visualization of articular cartilage using computed tomography: exploiting electrostatic interactions for improved sensitivity. J Am Chem Soc 2009;131:13234–5.
[11] Bansal PN, Joshi NS, Entezari V, Malone BC, Stewart RC, Snyder BD, Grinstaff MW. Cationic contrast agents improve quantification of glycosaminoglycan (GAG) content by contrast enhanced CT imaging of cartilage. J Orthop Res 2011;29(5):704–9.
[12] Silvast TS, Jurvelin JS, Aula AS, Lammi MJ, Toyras J. Contrast agent-enhanced computed tomography of articular cartilage: association with tissue composition and properties. Acta Radiol 2009;50(1):78–85.
[13] Lakin BA, Grasso DJ, Shah SS, Stewart RC, Bansal PN, Freedman JD, Grinstaff MW, Snyder BD. Cationic agent contrast-enhanced computed tomography imaging of cartilage correlates with the compressive modulus and coefficient of friction. Osteoarthr Cartil 2013;21(1):60–8.
[14] Lakin BA, Ellis DJ, Shelofsky JS, Freedman JD, Grinstaff MW, Snyder BD. Contrast enhanced CT facilitates rapid, non-destructive assessment of cartilage and bone properties of the human metacarpal. Osteoarthr Cartil 2015;23(12):2158–66.
[15] Stewart RC, Honkanen JTJ, Kokkonen HT, Tiitu V, Saarakkala S, Joukainen A, Snyder BD, Jurvelin JS, Grinstaff MW, Töyräs J. Contrast-Enhanced computed tomography enables quantitative evaluation of tissue properties at intrajoint regions in cadaveric knee cartilage. Cartilage 2017;8(4):391–9.
[16] Nickmanesh R, Stewart RC, Snyder BD, Grinstaff MW, Masri BA, Wilson DR. Contrast-enhanced computed tomography (CECT) attenuation is associated with stiffness of intact knee cartilage. J Orthop Res 2018(November 2017):1–26.
[17] Stewart RC, Bansal PN, Entezari V, Lusic H, Nazarian RM, Snyder BD, Grinstaff MW. Contrast-enhanced CT with a high-affinity cationic contrast agent for imaging ex vivo bovine, intact ex vivo rabbit, and in vivo rabbit cartilage. Radiology 2013;266(1):141–50.
[18] Wysokinski TW, Chapman DL, Adams G, Renier M, Suortti P, Thomlinson W. Beamlines of the biomedical imaging and therapy facility at the Canadian light source - Part 2. Nucl Instr Methods Phys Res A 2007;582:73–6.
[19] Wu G, Siegler S, Allard P, Kirtley C, Leardini A, Rosenbaum D, Whittle M, D'Lima DD, Cristofolini L, Witte H, Schmid O, Stokes I. ISB recommendation on definitions of joint coordinate system of various joints for the reporting of human joint motion—part I: ankle, hip, and spine. J Biomech 2002;35(4):543–8.
[20] Buchan LL. Open mri investigation of contact mechanics in cam femoroacetabular impingement by. University of British Columbia; 2015.
[21] Petersilge CA. Chronic adult hip pain: MR arthrography of the hip. RadioGraphics 2000;20(suppl_1):S43–52.
[22] Fedorov A, Beichel R, Kalpathy-Cramer J, Finet J, Fillion-Robin JC, Pujol S, Bauer C, Jennings D, Fennessy F, Sonka M, Buatti J, Aylward S, Miller JV, Pieper S, Kikinis R. 3D Slicer as an image computing platform for the quantitative imaging network. Magn Reson Imaging 2012;30(9):1323–41.
[23] Kang X, Zhang H, Garbuz D, Wilson DR, Hodgson AJ. Preliminary evaluation of an MRI-based technique for displaying and quantifying bony deformities in cam-type femoroacetabular impingement. Int J Comput Assist Radiol Surg 2013;8(6):967–75.
[24] Neumann G, Mendicuti AD, Zou KH, Minas T, Coblyn J, Winalski CS, Lang P. Prevalence of labral tears and cartilage loss in patients with mechanical symptoms of the hip: evaluation using MR arthrography. Osteoarthr Cartil 2007;15(8):909–17.
[25] Palmer AW, Guldberg RE, Levenston ME. Analysis of cartilage matrix fixed charge density and three-dimensional morphology via contrast-enhanced microcomputed tomography. Proc Natl Acad Sci 2006;103(51):19255–60.
[26] Stewart RC, Bansal PN, Snyder BD, Grinstaff MW. High-affinity cationic contrast agent for imaging ex vivo. Radiology 2013;266(1):141–50.
[27] J. DeCoster, "Testing group differences using t-tests, ANOVA, and nonparametric measures," Retrieved November 2018 from http//www.stat-help.com/notes.html, 2006.
[28] Kurrat HJ, Oberländer W. The thickness of the cartilage in the hip joint. J Anat 1978;126(Pt 1):145–55.
[29] Adam RPC, Eckstein F, Milz S. The distribution of cartilage thickness within the joints of the lower limb of elderly individuals. J Anat 1998;193:203–14.
[30] Stewart RC, Patwa AN, Lusic H, Freedman JD, Wathier M, Snyder BD, Guermazi A, Grinstaff MW. Synthesis and preclinical characterization of a cationic iodinated imaging contrast agent (CA4+) and its use for quantitative computed tomography of ex vivo human hip cartilage. J Med Chem 2017;60(13):5543–55.
[31] Bansal PN, Joshi NS, Entezari V, Grinstaff MW, Snyder BD. Contrast enhanced computed tomography can predict the glycosaminoglycan content and biomechanical properties of articular cartilage. Osteoarthr Cartil 2010;18(2):184–191.